Polarization-insensitive all-optical wavelength conversion of 320 Gb/s RZ-DQPSK signals using a Ti:PPLN waveguide

**H. Hu · R. Nouroozi · R. Ludwig · B. Huettl ·
C. Schmidt-Langhorst · H. Suche · W. Sohler ·
C. Schubert**

Abstract Polarization-insensitive wavelength conversion of a single channel 320 Gb/s RZ-DQPSK data signal using a Ti:PPLN waveguide in a bi-directional loop configuration with less than 0.5 dB polarization sensitivity is reported. The conversion efficiency with polarization scrambling of the signal was −21 dB, which includes 9.2 dB of passive losses in the whole Ti:PPLN subsystem. In BER measurements error-free operation with 2 dB OSNR penalty for the converted signal was achieved. Theoretical and experimental investigations of the temporal shape and chirp of the converted data pulses show only very little broadening and chirping, indicating the potential for wavelength conversion of even much higher data rates.

H. Hu was on leave from School of Electronic and Information Engineering, Tianjin University, Tianjin 300072, China.

H. Hu (✉) · R. Ludwig · B. Huettl · C. Schmidt-Langhorst ·
C. Schubert
Fraunhofer Institute for Telecommunications,
Heinrich-Hertz-Institut, Einsteinufer 37, 10587 Berlin, Germany
e-mail: huhao@fotonik.dtu.dk

C. Schubert
e-mail: colja.schubert@hhi.fraunhofer.de

Present address:
H. Hu
DTU Fotonik, Technical University of Denmark, Building 343,
2800 Kgs. Lyngby, Denmark

R. Nouroozi · H. Suche · W. Sohler
Faculty of Science, Applied Physics, University of Paderborn,
Paderborn, Germany

R. Nouroozi
e-mail: rahman.nouroozi@uni-paderborn.de

1 Introduction

All-optical wavelength conversion (AOWC) is a key function in future wavelength division multiplexing (WDM) networks [1]. It can offer advantages over optical-electrical-optical (O/E/O) schemes, such as a high signal bandwidth (far beyond 100 Gb/s), simultaneous conversion of several WDM channels as well as transparency to data rate and modulation format. Various techniques for wavelength conversion of high-speed data signals (320 Gb/s or beyond) have been demonstrated so far. They were mainly based on third-order non-linear effects or cascaded $\chi^{(2)}$ processes, such as cross phase modulation (XPM), four wave mixing (FWM) or cascaded second harmonic and difference frequency generation (cSHG/DFG) [2–7]. The non-linear media commonly used in these AOWCs were semiconductor optical amplifiers (SOA), highly non-linear fibers (HNLF) or periodically poled lithium niobate (PPLN) waveguides. AOWC using a SOA has been demonstrated up to 320 Gb/s [2], based on a filtered XPM-induced chirp. Because the XPM requires an amplitude-modulated signal, this scheme cannot be applied to phase modulated signals and is thus not transparent to the modulation format. AOWC using HNLF has been shown to operate up to 640 Gb/s, either using a filtered XPM-induced chirp as described above [3] or based on FWM [4, 5]. The XPM-based method is again not format transparent, but the FWM approach can be used for amplitude and phase modulated signals. AOWC using PPLN waveguides has been demonstrated up to 320 Gb/s based on either cSHG/DFG [6] or cascaded sum frequency generation (SFG) and DFG [7]. These schemes preserve the phase information and are therefore transparent to the modulation format.

Polarization insensitivity is an important feature for all-optical wavelength converters with respect to system

applications. Most of the non-linear effects used in the schemes mentioned above are inherently polarization dependent. Several approaches have been proposed so far to overcome this problem and to realize polarization insensitivity. For SOA-based AOWC a co-polarized pump scheme was proposed and demonstrated [8, 9]. In the case of HNLF or photonic crystal fiber (PCF), a similar co-polarized pump scheme was proposed [10, 11]. A polarization-diversity scheme with a bi-directional loop configuration was also demonstrated [12]. In addition, polarization-insensitive AOWC has been demonstrated at 160 Gb/s using XPM and subsequent optical filtering in a circular-birefringence highly non-linear fiber (CB-HNLF) [13]. Another technique is based on the depolarization in a dispersion-flattened PCF [14]. For AOWC-based on PPLN waveguides, a polarization-diversity loop with bi-directional operation has been demonstrated [15, 16]. A similar scheme is based on a double pass non-linear interaction in a PPLN waveguide [17].

The AOWC exploiting cSHG/DFG in a PPLN waveguide has attracted considerable research interests due to its ultra-fast response, negligible spontaneous emission noise, wide conversion range and the potential of high conversion efficiency [18–20].

In this paper, we report theoretical and experimental investigations of the temporal shape and chirp of the converted data pulses in Ti:PPLN wavelength converters. The broadening and chirping for input pulses of 1.4 ps FWHM is negligible allowing one to set up a polarization-insensitive PPLN subsystem for ultra-fast wavelength conversion. Operation with a single channel 320 Gb/s return-to-zero differential-quaternary-phase-shift-keying (RZ-DQPSK) data signal is demonstrated and analyzed in detail. To the best of our knowledge this is the highest operation speed of a polarization-insensitive wavelength converter based on a PPLN waveguide reported to date.

2 Polarization-insensitive wavelength conversion

As $\chi^{(2)}$-based non-linear optical wavelength conversion in PPLN is inherently polarization dependent, a diversity scheme processing the two polarization components independently is needed. Therefore, we used a ring configuration to convert both polarization components in the same device.

2.1 Principle of operation

To convert a signal in the telecom C-band by difference frequency generation (DFG) in a PPLN waveguide, a pump of $\sim$0.78 μm wavelength is required to fulfill energy conservation. This pump can be generated internally by quasi phase matched second harmonic generation (SHG) of a "fundamental" wave. Simultaneously with this process, the input
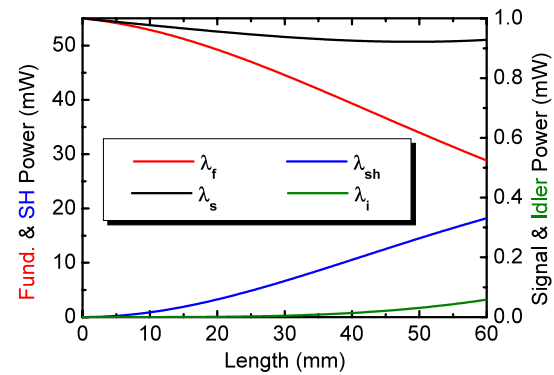

Fig. 1 Calculated evolution of fundamental (λ_f = 1546 nm), SH (λ_{sh} = 773 nm), signal (λ_s = 1551 nm), and idler (λ_i = 1541 nm) power levels along the waveguide for 55 mW of coupled fundamental power and 1 mW of coupled signal power
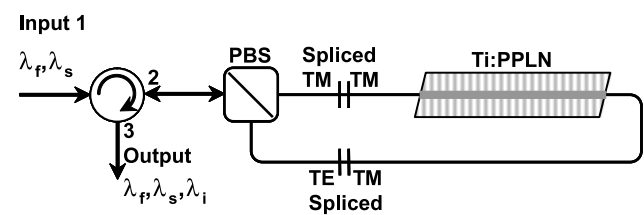

Fig. 2 Polarization insensitive PPLN subsystem

signal is (slightly) amplified by optical parametric amplification (OPA) and a wavelength-shifted idler is generated by quasi phase matched DFG, known as cascaded SHG/DFG (cSHG/DFG).

As an example, in Fig. 1 the calculated evolution of fundamental, SH, signal and idler power levels in a Ti:PPLN waveguide (see Sect. 3.1) is shown for cw operation. An effective interaction length of 60 mm, homogeneous quasi phase matching, 55 mW of coupled fundamental power and 1 mW of coupled signal power have been assumed. The fundamental wave is continuously depleted due to SHG. Simultaneously, the onset of OPA can be observed and the growth of an idler along the interaction length. The growth rate of the SH-wave is somewhat reduced due to simultaneous parametric amplification and wavelength conversion by DFG.

2.2 Polarization-diversity scheme

To provide a polarization-diversity scheme with an intrinsic equalization of the differential group delay [19], a polarization maintaining loop configuration with bi-directional operation of the wavelength converter is used (see Fig. 2). The two polarization components of fundamental and signal waves are routed by a polarization beam splitter (PBS) and polarization maintaining (PM) fibers contra-directionally through the Ti:PPLN waveguide. Appropriate splicing of the PM-fibers in the fiber loop guarantee that both polarization components pass the Ti:PPLN waveguide as TM-modes in

both directions. They are recombined together with the generated idler components by the PBS and routed to port 3 of the circulator.

The polarization of the fundamental wave at port 1 is adjusted for equal conversion efficiencies of the two polarization components minimizing the polarization dependent loss of the converted data in the PPLN subsystem.

3 Characteristics of the polarization-insensitive PPLN subsystem

3.1 Ti-diffused PPLN waveguide

The heart of the PPLN subsystem is a Ti-diffused (1060 °C, 8.5 hrs.) PPLN waveguide of 7 μm width and 80 mm length. Standard electric field poling with a domain periodicity of 16.4 μm was applied to achieve quasi phase matching in the C-band at elevated temperatures; high temperature operation (∼180 °C) was used to avoid optically induced changes of the index of refraction ("optical damage"). The waveguide propagation losses at 1550 nm wavelength are ∼0.1 dB/cm (for TM-polarization). The end facets of the waveguide are angle polished under 5.8° and AR-coated to avoid Fabry–Perot effects. The sample is mounted on a copper base plate to enable homogeneous heating and a precise temperature control.

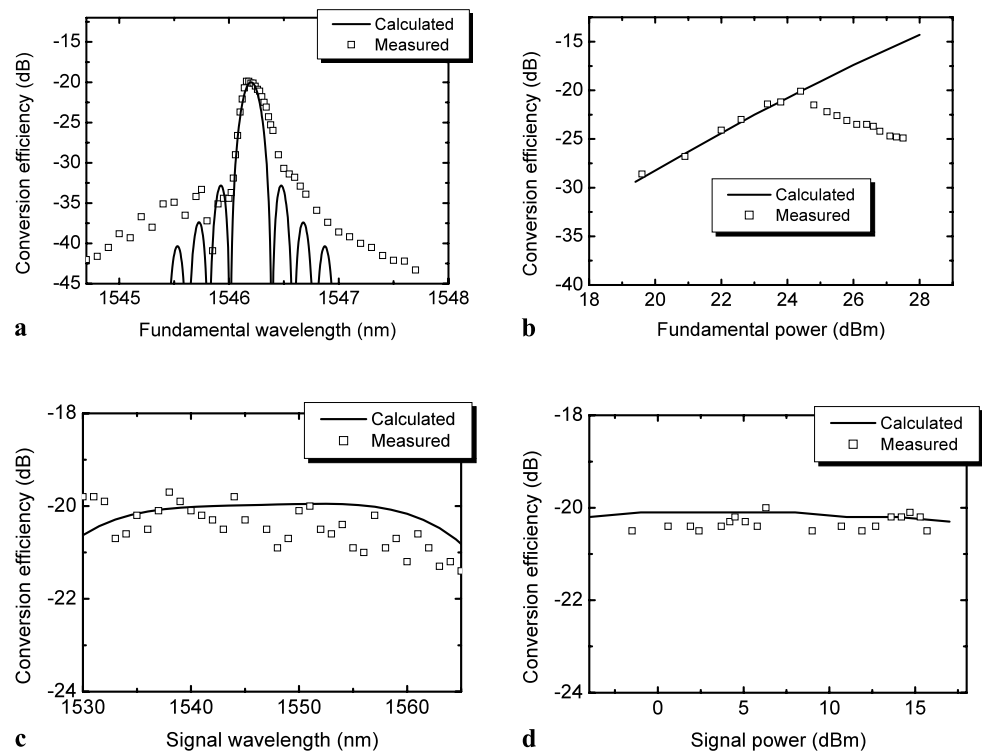Single-mode polarization maintaining fiber (PMF) pigtails with angled and AR-coated ferrules are aligned to the

Ti:PPLN waveguide using built-in micromanipulators. The total loss of the PPLN subsystem including coupling loss, circulator and PBS is 9.2 dB.

3.2 Wavelength conversion of cw signals

Using cw sources for fundamental and signal waves, the dependence of the conversion efficiency on the fundamental wavelength, signal wavelength, fundamental power and signal power was experimentally investigated and compared with modeling results. We define the external conversion efficiency as the ratio of the output power of the converted signal at port 3 and the input power of the signal at port 1, which includes the passive losses of the PPLN subsystem. The intrinsic conversion efficiency of the PPLN waveguide can be obtained by subtracting the passive losses of 9.2 dB.

Figure 3(a) shows the relation between the conversion efficiency and the fundamental wavelength. The signal wavelength is set to 1551 nm and the fundamental power is kept at 24.4 dBm (at input port 1) while tuning the wavelength. The maximum external conversion efficiency of −20.1 dB (internally −10.9 dB) is achieved at a fundamental wavelength of 1546.2 nm. The full width at half maximum (FWHM) of the measured curve is 0.22 ±0.02 nm, indicating that the fundamental wavelength needs to be set precisely within 0.1 nm. This FWHM is determined by an effective interaction length of 60 mm. The simulation results shown in Fig. 3 are based on this figure. Figure 3(b) shows the relation between the

Fig. 3 (**a**) Conversion efficiency vs. fundamental wavelength; (**b**) Conversion efficiency vs. fundamental power; (**c**) Conversion efficiency vs. signal wavelength; (**d**) Conversion efficiency vs. signal power. For the simulations an effective interaction length of 60 mm was assumed

conversion efficiency and the fundamental power. The fundamental wavelength is kept at 1546.2 nm while the power is changed. The maximum external conversion efficiency of −20.1 dB is achieved at a fundamental power of 24.4 dBm. For higher fundamental powers the conversion efficiency decreased as a result of the onset of photorefractive effects in the Ti:PPLN waveguide, which could be counteracted by tuning the fundamental wavelength. The simulation results indicate that higher conversion efficiencies can be expected for higher fundamental powers.

The relation between the conversion efficiency and the signal wavelength is shown in Fig. 3(c). The fundamental wavelength is 1546.2 nm and the fundamental power is 24.4 dBm. The result shows that the conversion efficiency is almost constant over the whole C band, which allows wavelength conversion of a high bandwidth signal or the simultaneous conversion of several WDM channels. Figure 3(d) shows the relation between the conversion efficiency and the signal power. The fundamental power and wavelength are set to 24.4 dBm and 1546.2 nm, respectively. The result shows that the conversion efficiency is almost constant for different signal power levels, which demonstrates the large input dynamic range (more than 17 dB) of the PPLN subsystem. For all four graphs, shown in Fig. 3, the simulations are in good agreement with the measured results.

3.3 Wavelength conversion of short signal pulses

In this section cSHG/DFG-based wavelength conversion of short signal pulses in a Ti:PPLN waveguide is discussed. To explore the limitations of this process to the conversion of ∼1.4 ps signal pulses, as used in high data rate transmission experiments with of 320 Gb/s RZ/DQPSK data (see Sect. 4), wavelength conversion of a train of short signal pulses of ∼1.4 ps halfwidth was investigated experimentally and theoretically.

Propagation and interaction of short optical pulses in a dispersive medium like $LiNbO_3$ in general cause additional effects like group velocity mismatch (GVM) and group velocity dispersion (GVD) leading to temporal walk off, thereby changing the shapes of the interacting pulses. These effects require the consideration of temporal first and second order derivatives in the governing equations [21]. We used the split step integration in time and frequency domains to solve the coupled amplitude equations in the slowly varying envelope approximation [21]. As an example, Fig. 4 shows the temporal evolution of the shapes of signal and idler pulses after transmission through 20, 40 and 60 mm of the waveguide. To approximately model the system experiments, an input signal pulse of 100 mW peak power and 1.4 ps FWHM was assumed (λ_s = 1551 nm). The cw power level of the fundamental wave at λ_f = 1546.2 nm was 55 mW. Simulation results show negligible pulse broadening and walk off for the transmitted signal; also the pulse
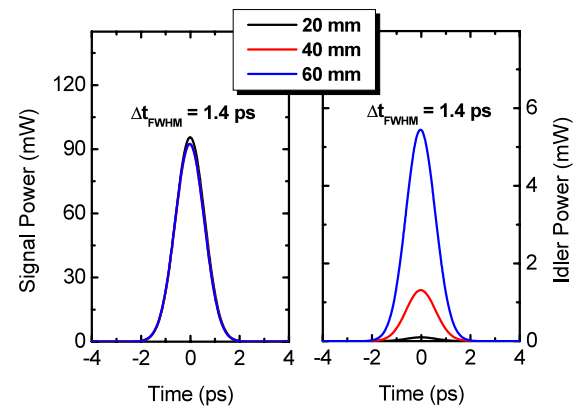

Fig. 4 Calculated evolution of the signal (λ_s = 1551 nm, left) and idler (λ_i = 1541.4 nm, right) pulses for cSHG/DFG-based wavelength conversion over a distance of 60 mm long effective interaction length are shown after 20 mm (*black*), 40 mm (*red*) and 60 mm (*blue*), respectively. The distortions of signal and idler pulses are negligible
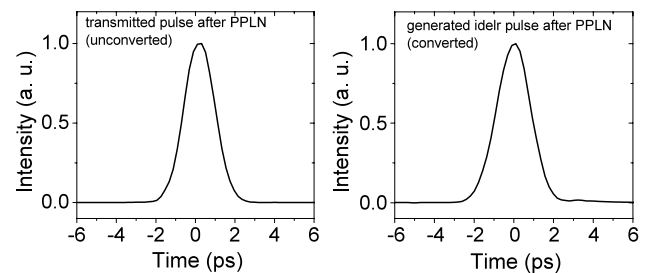

Fig. 5 Measured transmitted signal (*left*) and generated idler (*right*) pulses behind the PPLN subsystem. A small broadening of the wavelength shifted pulse is observed. In comparison with the input signal pulse of 1.65 ps FWHM also a small broadening of the transmitted signal pulse was observed

peak power remains nearly constant as propagation losses are partly compensated by parametric amplification (Fig. 4, left). The idler pulse (λ_i = 1541.4 nm) strongly grows with increasing interaction length; by comparing its peak power after 60 mm interaction length with the peak power of the input signal pulse, an internal conversion efficiency of ∼6% can be deduced. Moreover, the shape of the idler pulse at the output is practically identical with the shape of the signal pulse at the input (Fig. 4, right). In other words, the wavelength conversion by cSHG/DFG in 60 mm long Ti:PPLN waveguides induces only negligible distortions of 1.4 ps long pulses. A very weak, almost parabolic time-dependent phase chirp of less than 0.008 rad for signal and idler pulses are predicted leading to a very small positive frequency chirp for the signal and a negative (phase conjugation) for the idler pulses.

The corresponding experimental results are shown in Fig. 5. A small broadening of transmitted signal and idler pulses was observed. The original pulse width of 1.65 ps (FWHM, after some dispersive components (see Fig. 6) and in front of the PPLN subsystem) is broadened to 1.75 ps
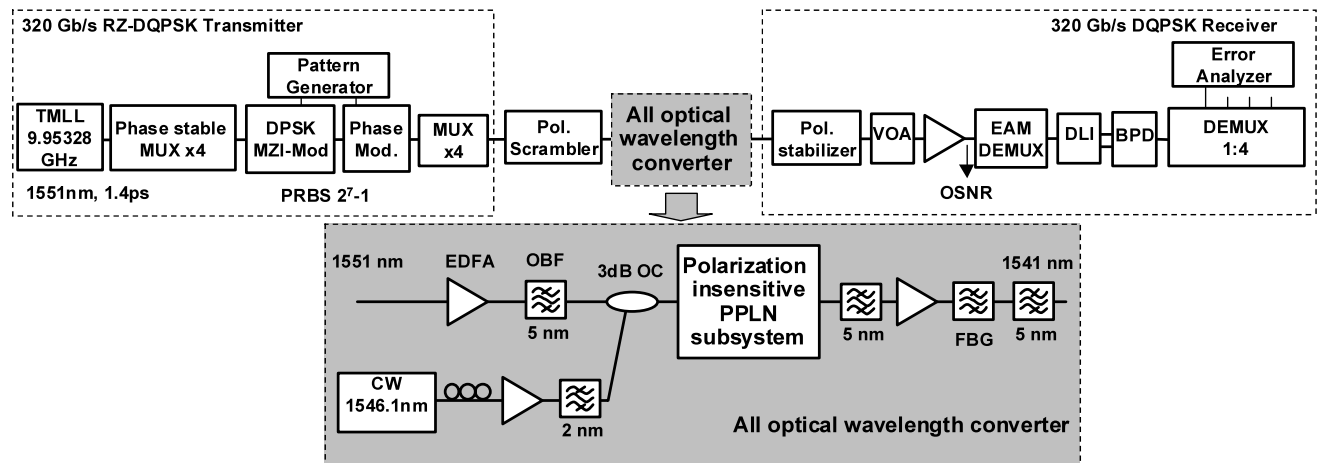
Fig. 6 Experimental setup for polarization insensitive all-optical wavelength conversion of 320 Gb/s RZ-DQPSK signals

for the signal and 1.8 ps for idler pulses, respectively, at the output of the Ti:PPLN subsystem. Moreover, only a small parabolic phase change for the signal and idler pulses (<0.15 rad) were found by frequency resolved optical gating (FROG) measurements indicating an almost linear frequency chirp, which can simply be compensated by dispersion compensating optical fiber.

Moreover, the propagation of even shorter pulses of 140 fs FWHM was theoretically investigated. In this case, a more significant broadening of the signal pulses ($\lambda_s = 1551$ nm) to ~200 fs—after transmission through the 60 mm long Ti:PPLN waveguide—was evaluated; this is mainly attributed to GVD. On the other hand, the wavelength-shifted idler pulses ($\lambda_i = 1541.4$ nm) broaden (parameter dependent) to ~150 fs only; this is again mainly a consequence of the GVD of the waveguide broadening the signal pulses but narrowing the idler pulses after spectral inversion. In addition, this partial compensation is influenced by the parameters of the non-linear wavelength conversion in the device. And further propagation in the waveguide without non-linear interaction (i.e. in a waveguide section without periodic domain grating) should lead to restored idler pulses at the output very similar to the input signal pulses. In other words, it should be possible to design PPLN wavelength converters even for very short pulses, which induce practically no pulse distortions and, therefore, do not lead to a limitation of the bit rate in communication systems. We anticipate, that ultra-fast PPLN wavelength converters can be designed for bit rates surpassing 3 Tbit/s.

4 Wavelength conversion of DQPSK data

The wavelength conversion scheme we used in the experiments is based on the cascaded SHG/DFG in the polarization-insensitive PPLN subsystem. It preserves the phase information and is transparent to the modulation format. In principle, it can also be used to convert polarization multiplexed signals since a polarization-diversity scheme is applied [15]. In our experiment, we demonstrate polarization-insensitive 320 Gb/s RZ-DQPSK wavelength conversion.

4.1 Experimental setup

The experimental setup for the polarization-insensitive all-optical wavelength conversion experiment is shown in Fig. 6. It included a 320 Gb/s RZ-DQPSK transmitter, the all-optical wavelength converter and a 320 Gb/s DQPSK receiver. The RZ-DQPSK transmitter consisted of a pulse source, a 10 GHz-to-40 GHz phase stable pulse multiplier, a DQPSK modulator and a 40 Gbaud to 160 Gbaud optical time division multiplexer. The pulse source was a tunable semiconductor mode locked laser (TMLL), which produced a 1.4 ps, 10 GHz (STM-64) optical pulse train at 1551 nm, multiplied to 40 GHz with a passive phase stable multiplexer. A two-stage modulator was used to encode the DQPSK signal. The first stage was a Mach-Zehnder LiNbO$_3$ device driven in push-pull mode by a 40 Gb/s PRBS signal ($2^7 - 1$) from a pattern generator to encode the π phase shift. The second stage was a LiNbO$_3$ phase modulator to encode the additional $\pi/2$ phase shift, driven by the same electrical signal with a sufficient delay for de-correlation. The modulated 40 Gbaud (80 Gb/s) RZ-DQPSK signal was then multiplexed in time by a passive fiber-delay multiplexer (MUX ×4) to generate a 160 Gbaud (320 Gb/s) RZ-DQPSK signal.

In the wavelength converter the generated 320 Gb/s RZ-DQPSK signal was amplified by an EDFA, then filtered by a 5 nm wide optical bandpass filter (OBF) and finally launched into the polarization-insensitive PPLN subsystem through a 3 dB coupler (OC). The signal power was

15.1 dBm at the input of the polarization-insensitive PPLN subsystem. The CW fundamental light at 1546.2 nm was amplified by a high-power EDFA, filtered and launched into the polarization-insensitive PPLN subsystem through the second input of the 3 dB coupler. The fundamental power was 24.4 dBm at the input of the polarization-insensitive PPLN subsystem.

The polarization controller in front of the EDFA was adjusted for polarization-insensitive conversion efficiency. At the output of the polarization-insensitive PPLN subsystem the signal was launched into a filtering subsystem, which consisted of two 5 nm wide OBFs, an EDFA in between and a tunable fiber Bragg grating (FBG). The FBG was used to block the fundamental wave, and the OBFs separated the converted signal at 1541 nm from the fundamental and the original signal waves. The polarization of the data signal was scrambled in front of the converter, to test the polarization insensitivity. In the DQPSK receiver a polarization stabilizer was used to de-scramble the converted data signal in order to mitigate the polarization sensitivity of the receiver.

The 320 Gb/s RZ-DQPSK receiver consisted of an optical pre-amplification stage, an electro-absorption modulator (EAM) as demultiplexer, a delay line interferometer (DLI), a balanced photo-detector (BPD), directly attached to an electrical 1:4 demultiplexer and an error analyzer. The EAM demultiplexer was used to select one of the four 80 Gb/s (40 Gbaud) OTDM tributaries. The DLI had a free spectral range of 40 GHz and was used to demodulate the I or Q channel from the demultiplexed 80 Gb/s DQPSK signal. Since no DQPSK pre-coder was used in the transmitter, the EAM was programmed to the expected bit pattern, which limited the word length in our experiments to $2^7 - 1$. We used a variable optical attenuation (VOA) at the receiver input to vary the received optical signal to noise ratio (OSNR).

4.2 Experimental results

The spectrum at the input and the output of the polarization-insensitive PPLN subsystem is shown in Fig. 7(a). The conversion efficiency for the 320 Gb/s RZ-DQPSK signal with polarization scrambling is −21 dB. It could be improved if the total insertion loss of the PPLN subsystem including the fiber-optic components would be reduced. Nevertheless, the internal efficiency of about −11 dB (see Fig. 7(a)) is in good agreement with theoretical calculations assuming 17.4 dBm of fundamental power launched in each direction into the PPLN waveguide. The spectrum of the wavelength-converted signal at 1541 nm after filtering is shown in Fig. 7(b). The fundamental light is well suppressed by the FBG notch filter. The power of the residual fundamental and the original signal are 28 dB lower compared to the wavelength-converted signal.

To characterize the residual polarization sensitivity of the PPLN subsystem we measured the power of the converted
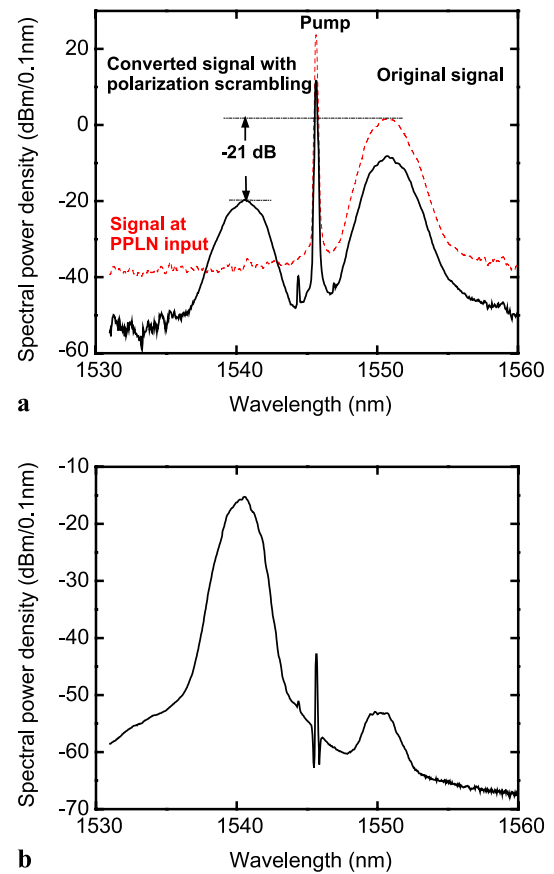

Fig. 7 (**a**) Spectrum at the input and the output of the AOWC. (**b**) The output spectrum of the wavelength converted signal after filtering
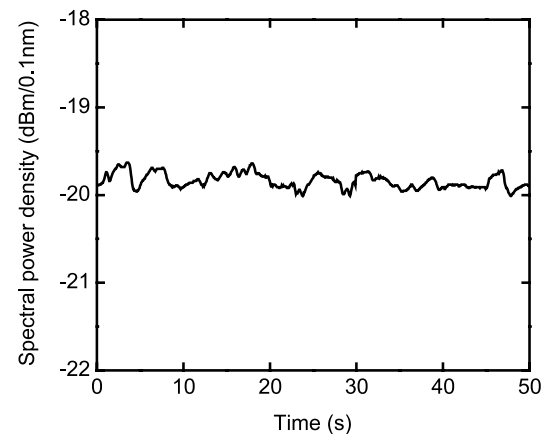

Fig. 8 Power fluctuation of the converted signal with polarization scrambling

signal versus time (50 s) with slow polarization scrambling (using a motorized polarization controller with a scan-rate of 0.08 Hz). The maximum fluctuation was less than 0.5 dB, as shown in Fig. 8.

The results of the BER measurements are shown in Fig. 9(a) as a function of the OSNR at the 320 Gb/s

DQPSK receiver. BER curves are plotted for the 320 Gb/s DQPSK signal back-to-back before conversion (wavelength 1551 nm), and for the converted 320 Gb/s DQPSK signal with and without polarization scrambling (wavelength 1546 nm). Polarization-insensitive 320 Gb/s RZ-DQPSK wavelength conversion is successfully achieved with an error-free performance (BER 10^{-9}). The wavelength conversion causes 2-dB OSNR penalty at the BER of 10^{-9} compared with the back-to-back case (unconverted signal). The penalty is partly due to the different sensitivity of the receiver for the different wavelengths of the unconverted and converted signal. However, the results indicate that the additional penalty caused by the polarization scrambling is negligible. The measurements shown in Fig. 9(a) are made for a single tributary (best channel). All tributary channels were measured and the variation of the received power required for BER $= 10^{-9}$ was found to be less than 1 dB. The 40 Gb/s eye-diagrams of the wavelength converted, demultiplexed and demodulated signal (BER $= 10^{-9}$) without and with polarization scrambling are shown in Fig. 9(b) and (c), respectively. The eye-diagrams indicate again, that the wavelength-converted signals with and without polarization scrambling have almost identical performance.

5 Conclusions

We have demonstrated polarization-insensitive 320 Gb/s RZ-DQPSK wavelength conversion using a Ti:PPLN waveguide in a polarization-diversity scheme. Less than 0.5 dB polarization sensitivity was obtained. Error-free operation with 2 dB OSNR penalty for the converted signal was achieved using a polarization scrambled input data signal. In addition, we investigated the characteristics of the polarization-insensitive PPLN subsystem. The results show that the conversion efficiency of the AOWC is almost constant over the whole C-band and that the AOWC has a large input signal power dynamic range of more than 17 dB. The conversion efficiency for the 320 Gb/s RZ-DQPSK signal with polarization scrambling is -21 dB, which includes the passive losses of the PPLN subsystem. The BER measurements and eye-diagrams show that the wavelength-converted signals with and without polarization scrambling in front of the AOWC have identical performance.

Theoretical and experimental investigations of the temporal shape and chirp of the converted data pulses show only very little broadening and chirping indicating the potential for wavelength conversion of even much higher data rates. This is confirmed by modeling calculations of signal and idler pulse evolution of even shorter pulsewidth. They reveal that pulse broadening of the signal pulses induced by group velocity dispersion can already be compensated to a large degree in the device itself as a consequence of the spectral
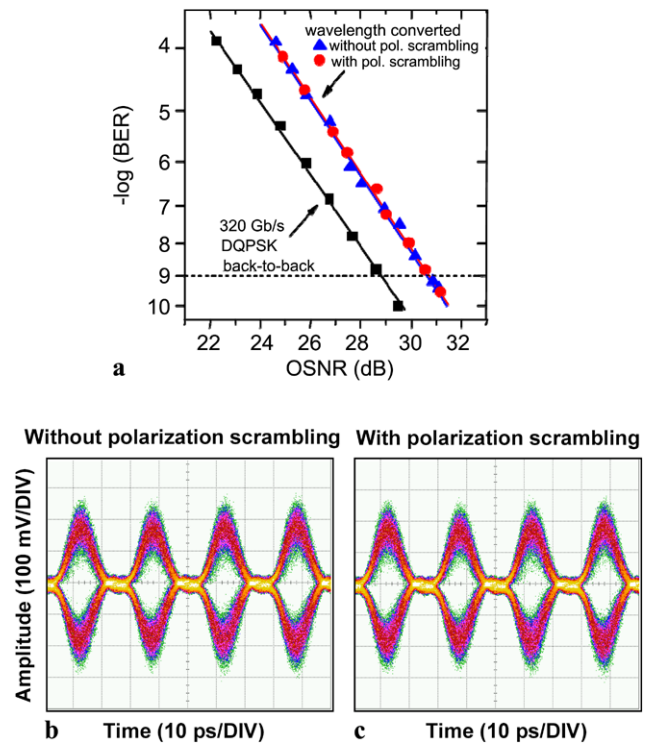

Fig. 9 (**a**) BER measurements for the 320 Gb/s DQPSK signal back-to-back, and for the converted 320 Gb/s DQPSK signal with and without polarization scrambling. (**b**) and (**c**) 40 Gb/s eye-diagram of the wavelength converted, demultiplexed, and demodulated signal in the DQPSK receiver without and with polarization scrambling

inversion of the wavelength-shifted idler. We anticipate, that ultra-fast Ti:PPLN wavelength converters can be designed for bit rates surpassing 3 Tbit/s.

References

1. S.J.B. Yoo, J. Lightwave Technol. **14**, 955 (1996)
2. Y. Liu, E. Tangdiongga, Z. Li, H. de Waardt, A.M.J. Koonen, G.D. Khoe, X. Shu, I. Bennion, H.J.S. Dorren, J. Lightwave Technol. **25**, 103 (2007)
3. M. Galili, L.K. Oxenlowe, H.C.H. Mulvad, A.T. Clausen, P. Jeppesen, IEEE J. Sel. Top. Quantum Electron. **14**, 573 (2008)
4. M. Galili, H.C.H. Mulvad, L. Gruner-Nielsen, J. Xu, L.K. Oxenlowe, A.T. Clausen, P. Jeppesen, in *European Conference on Optical Communication, ECOC 2008*, Brussels, Belgium (2008), p. Paper Tu.3.D.5
5. H. Hu, E. Palushani, M. Galili, H.C.H. Mulvad, A. Clausen, L.K. Oxenløwe, P. Jeppesen, Opt. Express **18**, 9961 (2010)
6. J. Sun, W. Liu, J. Tian, J.R. Kurz, M.M. Fejer, IEEE Photonics Technol. Lett. **15**, 1743 (2003)
7. A. Bogoni, Xiaoxia Wu, I. Fazal, A.E. Willner, in *Conference on Optical Fiber Communication, OFC 2009*, San Diego, USA (2009), p. Paper OThS5
8. C. Porzi, A. Bogoni, L. Poti, G. Contestabile, IEEE Photonics Technol. Lett. **17**, 633 (2005)
9. J.P.R. Lacey, M.A. Summerfield, S.J. Madden, J. Lightwave Technol. **16**, 2419 (1998)

10. J. Yu, M.-F. Huang, N. Cvijetic, in *Conference on Optical Fiber Communication, OFC 2009*, San Diego, USA (2009), p. Paper OThS7
11. J. Ma, J. Yu, C. Yu, Z. Jia, X. Sang, Z. Zhou, T. Wang, G.K. Chang, J. Lightwave Technol. **24**, 2851 (2006)
12. K.K. Chow, C. Shu, C. Lin, A. Bjarklev, IEEE Photon. Technol. Lett. **17**, 624 (2005)
13. T. Tanemura, J. Lee, D. Wang, K. Katoh, K. Kikuchi, Opt. Express **14**, 1408 (2006)
14. T. Yang, C. Shu, C. Lin, Opt. Express **13**, 5409 (2005)
15. V. Pusino, P. Minzioni, I. Cristiani, V. Degiorgio, L. Marazzi, P. Boffi, M. Ferrario, P. Martelli, P. Parolari, A. Righetti, R. Siano, M. Martinelli, C. Langrock, M.M. Fejer, in *Conference on Optical Fiber Communication, OFC 2009*, San Diego, USA (2009), p. Paper OThS3
16. H. Hu, H. Suche, R. Ludwig, B. Huettl, C. Schmidt-Langhorst, R. Nouroozi, W. Sohler, C. Schubert, in *Conference on Optical Fiber Communication, OFC 2009*, San Diego, USA (2009), p. Paper OThS6
17. I. Cristiani, V. Degiorgio, L. Socci, F. Carbone, M. Romagnoli, IEEE Photon. Technol. Lett. **14**, 669 (2002)
18. S.L. Jansen, D. van den Borne, P.M. Krummrich, S. Spalter, G.-D. Khoe, H. de Waardt, IEEE J. Sel. Top. Quantum Electron. **12**, 505 (2006)
19. M.H. Chou, K.R. Parameswaran, M.M. Fejer, I. Brener, IEICE Trans. Electron. **E83C**, 869 (2000)
20. C. Langrock, S. Kumar, J. E McGeehan, A.E. Willner, M.M. Fejer, J. Lightwave Technol. **24**, 2579 (2006)
21. W. Gründkötter, Ph.D. thesis, University of Paderborn (2008)